

Sparse Spatial Transformers for Few-Shot Learning

Haoxing Chen, Huaxiong Li, Yaohui Li, Chunlin Chen

Department of Control and Systems Engineering, Nanjing University, Nanjing, China

{haoxingchen, yaohuili}@smail.nju.edu.cn, {huaxiongli, clchen}@nju.edu.cn

Abstract

Learning from limited data is a challenging task since the scarcity of data leads to a poor generalization of the trained model. The classical global pooled representation is likely to lose useful local information. Recently, many few shot learning methods address this challenge by using deep descriptors and learning a pixel-level metric. However, using deep descriptors as feature representations may lose the contextual information of the image. And most of these methods deal with each class in the support set independently, which cannot sufficiently utilize discriminative information and task-specific embeddings. In this paper, we propose a novel Transformer based neural network architecture called Sparse Spatial Transformers (SSFormers), which can find task-relevant features and suppress task-irrelevant features. Specifically, we first divide each input image into several image patches of different sizes to obtain dense local features. These features retain contextual information while expressing local information. Then, a sparse spatial transformer layer is proposed to find spatial correspondence between the query image and the entire support set to select task-relevant image patches and suppress task-irrelevant image patches. Finally, we propose an image patch matching module to calculate the distance between dense local representations to determine which category the query image belongs to in the support set. Extensive experiments on popular few-shot learning benchmarks show that our method achieves the state-of-the-art performance. Our code is available at <https://github.com/chenhaoxing/SSFormers>.

1. Introduction

With the availability of large-scale labeled data, visual understanding technology has made great progress in many tasks [1, 15, 28]. However, collecting and labeling such a large amount of data is time-consuming and laborious. Few-shot learning is committed to solving this problem, which enables deep models to have better generalization ability even on a small number of samples.

Recently, many few-shot learning methods have been proposed, which can be roughly divided into two categories: meta-learning [7, 18, 5] and metric-learning [25, 22, 23, 13, 2, 3]. The goal of meta-learning is to learn how to deal with new tasks in the process of learning multiple tasks. Metric learning focuses on learning a good feature representation or relation measure.

For feature representations, most of the existing metric-learning based methods [25, 22, 12] adopt global features for recognition, which may cause useful local information to be lost and overwhelmed. Recently, DN4 [13], MATANet [2] and DeepEMD [27] adopt dense feature representations (i.e., deep descriptors) for few-shot learning tasks, which have been verified to be more expressive and effective than using global features. And another branch that enhances image representation uses the attention mechanism to align the query image with the support set. For example, Cross Attention Network (CAN) [10] and SAML [9] use the semantic correlation between the support set and query image to highlight the target object.

For the relation measure, existing dense feature based methods usually adopt a pixel-level metric and the query image is taken as a set of deep descriptors. For example, in DN4 [13], for each query deep descriptor, they find its nearest neighbor descriptors in each support class. Also, CovaMNet [14] calculates a local similarity between each query deep descriptor and a support class by a covariance metric.

However, most existing methods use global features or deep descriptors, and they are not effective for few-shot image classification. Due to the global feature lose local information, and deep descriptors lose the contextual information of the image. Moreover, the above methods all process each support class independently, and cannot use the context information of the entire task to generate task-specific features.

In this paper, we propose a novel sparse spatial transformer (SSFormers), which extracts the spatial correlation between the query image and the current task (the entire support set), aiming to align task-relevant image patches and suppress task-irrelevant image patches. First, we di-

vide each input image into several patches and get dense local features. Second, we select task-relevant query patches by a two-way selection function, i.e., mutual nearest neighbour [8, 16]. And use selected query patches to align support classes. Finally, a patch matching module is proposed to measure the similarity between query images and aligned support classes. For each patch from a query image, the patch matching module calculates its similarity scores to the nearest neighbor patch in each aligned class prototype. Then, similarity scores from all query patches are accumulated as a patch-to-class similarity.

The main contributions of this work are summarized as follows:

- 1) We propose a novel *sparse spatial transformers* for few-shot learning, which can select task-relevant patches and generate a task-specific prototype.
- 2) We propose a *patch matching module* to get similarity between query images and task-specific prototypes. Experiments prove that it is more suitable for image patch-based feature representation than directly using the cosine similarity.
- 3) We conduct extensive experiments on popular few-shot learning benchmarks and show that the proposed model achieving competitive results compared to other state-of-the-art methods.

2. Related Work

Global Feature based Methods. The traditional metric-learning based few-shot learning methods use an additional global average pooling (GAP) layer to obtain the global feature representation at the end of the backbone and utilize different metrics for classification. MatchingNet [25] utilizes the cosine distance to measure the similarity between the query image and each support class. ProtoNet [22] takes the empirical mean as the prototype representation of each category and uses Euclidean distance as the distance metric. RelationNet [23] proposed a non-linear learnable distance metric. These methods based on global features will lose a lot of useful local information, which is harmful to classification tasks under few-shot learning settings.

Dense Feature based Methods. Another branch of metric-learning based methods uses pixel-level deep descriptors as feature representations. DN4 [13] uses the k -nearest neighbor algorithm to obtain the pixel-level similarity between images. MATANet [2] proposes a multi-scale task adaptive network to select task-relevant deep descriptors at multiple scales. DeepEMD [27] proposes a differentiable earth mover’s distance to calculate the similarity between image patches. Our SSFormers also belong to this method based on dense features. A major difference in our method is that we divide input images into several patches of different

sizes and extract features. Compared with global features, the features extracted by our method can express local information. And compared with deep descriptors, the extracted features contain context information.

Attention based Methods. CAN [10] proposes a cross-attention algorithm to highlight the common objects in the image pair. SAML [9] proposes a collect and select strategy to align the main objects in the image pair. CrossTransformers [6] proposes to use a self-supervised learning algorithm to enhance the feature representation ability of the pre-trained backbone, and use a transformer to achieve alignment. SSFormers also be treated among the family of attention-based methods as they also aligned query images and support sets. Differently, our SSFormers select task-relevant patches in the query image to align support set to query image by a sparse spatial cross attention algorithm.

3. Preliminary

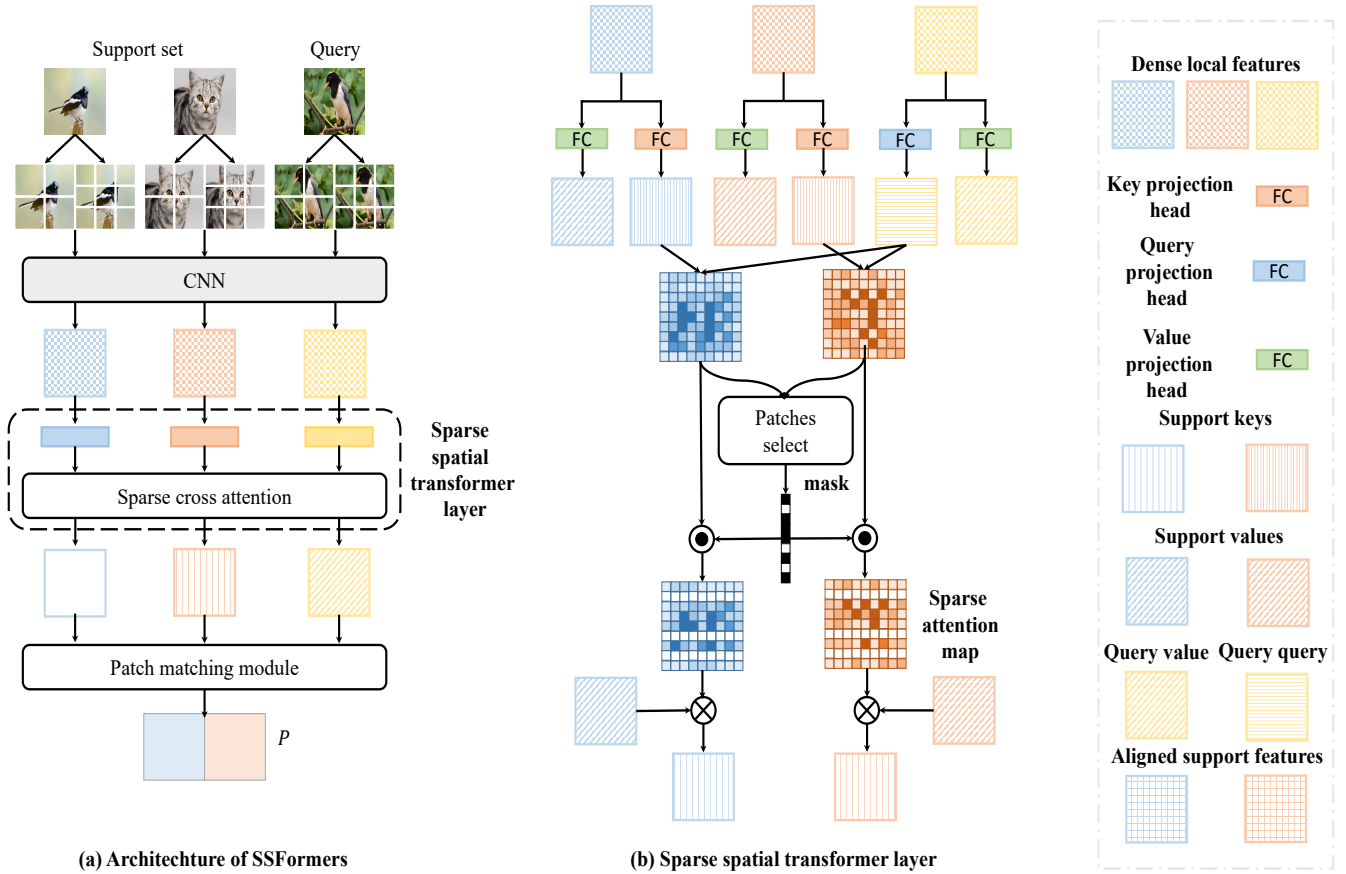
Before presenting our method in detail, we first introduce the problem definition of few-shot learning. Few-shot learning is dedicated to learning transferable knowledge between tasks and using the learned knowledge to solve new tasks. In the few-shot learning scenario, the task is usually set in the form of N -way M -shot, where N is the number of categories and M is the number of labeled samples in each category. Under this setting, the model is trained on a training set \mathcal{D}_{train} with a large amount of labeled data. To learn transferable knowledge, we use episodic training mechanisms to train our model. The episodic training mechanism samples batched tasks from \mathcal{D}_{train} for training. In each episode, we first construct query set $\mathcal{D}_Q = \{(x_i^q, y_i^q)\}_{i=1}^{N \times B}$ and support set $\mathcal{D}_S = \{(x_i^s, y_i^s)\}_{i=1}^{N \times M}$, where B is a hyperparameter that we need to fix in our experiments. Then our model predicts which support set category each sample in the query set belongs to. When the model training is complete, we sample tasks from unlabeled test sets \mathcal{D}_{test} to verify the performance of the model.

4. Our Method

In this section, we first introduce our method for generating dense local representations. Then we describe our sparse spatial transformers layer, which spatially aligns query images and support classes. Finally, we describe the patch matching module (PMM), which is used to calculate the final similarities. The overview of our framework is shown in Figure 1.

4.1. Dense Local Feature Extractor

The metric-learning based few-shot learning method aims to find an effective feature representation and a good distance metric to calculate the similarity between images. Different from the methods that use global features, local



(a) Architecture of SSFormers

(b) Sparse spatial transformer layer

Figure 1. Illustration of the proposed SSFormers. We propose to generate dense local features and finding task-relevant features by a sparse spatial transformers layer.

representation based methods have achieved better results because the local representation contains richer and more transferable semantic information. The difference from previous work is that our SSFormers aim to establish hierarchical local representations for spatial comparison.

As illustrated in Figure 1, dense local representations extractor F_θ evenly divides the image into $H \times W$ patches, and each image patch is individually encoded by the backbone network to generate a feature vector. The feature vectors generated by all patches constitute the dense local representations set of each image. To generate hierarchical local representations, we adopt a pyramid structure in the experiments. Thus the feature representation of an input image x can be denoted as $F_\theta(x) \in \mathbb{R}^{K \times C}$, where C is the number of channels, and K is the number of all local patch representations. Specifically, we adopt two image patch division strategies of size 2×2 and 3×3 to obtain 13 dense local representations.

In each N -way M -shot few-shot image recognition task, for each support class, we have M samples and get M feature representations. Instead of using empirical mean of M

feature representations [22] to obtain the class representation, we utilize all the patches in each support class, i.e., $S_n \in \mathbb{R}^{MK \times C}$, where S_n is the class representation of the n -th support class. The entire support set representation can be denoted as $S \in \mathbb{R}^{N \times MK \times C}$. Similarly, for a query image x_q , through F_θ , we can get feature representation $q = F_\theta(x_q) \in \mathbb{R}^{K \times C}$.

4.2. Sparse Spatial Transformers Layer

Sparse spatial transformers aim to enhance the discriminant ability of local feature representations by modeling the interdependencies between different patches in the query image and the entire support set. In a N -way M -shot task, key k_S and value v_S are generated for support set feature S using two independent linear projection: the key projection head $h_k: \mathbb{R}^C \mapsto \mathbb{R}^{C'}$ and the value projection head $h_v: \mathbb{R}^C \mapsto \mathbb{R}^{C'}$. Similarly, the query image feature q is embedded using the value projection head h_v and another the query projection head $h_q: \mathbb{R}^C \mapsto \mathbb{R}^{C'}$ to obtain value v_q and query q_q .

We argue that if the patch with the closest semantic dis-

tance to patch q_i is S_j , and the patch with the closest semantic distance to patch S_j is q_i , then they are likely to have the same local feature, where $q_i \in q_q, i \in \{1, \dots, K\}$ and $S_j \in k_S, j \in \{1, \dots, NMK\}$. On the other hand, if the closest patch of patch S_j is not q_i , then even if the closest descriptor of q_i is S_j , the actual relationship between them is relatively weak. In other words, the correlation between two patches is a function of mutual perception, not a function of one-way perception. Therefore, we can use this bidirectionality to select task-relevant patches in the current task.

We first calculated semantic relation matrix between query image and each support class n , and get \mathbf{R}_n :

$$\mathbf{R}_n = \frac{q_q \times k_{S_n}^\top}{\sqrt{C'}} \in \mathbb{R}^{K \times MK} \quad (1)$$

To finding task-relevant patches, we concatenate all semantic relation matrixes $\mathbf{R}_n, n = \{1, \dots, N\}$ to get $\mathbf{R} \in \mathbb{R}^{K \times NMK}$. Each row in \mathbf{R} represents the semantic similarity of each patch in the query image to all patches of all images in the support set.

Specifically, we propose a novel sparse spatial cross attention algorithm to find task-relevant patches in the query image. For each patch $q_i \in q_q$, we find its nearest neighbor n_q^i in k_S , and then find the nearest neighbor n_S^i of n_q^i in q_q . If $i = n_S^i$, then we consider q_i to be a task-relevant patch. After collecting all task-relevant patches in q_q , we can get the mask $m = [m_1; \dots; m_K]$, which can be computed as:

$$n_q^i = \arg \max_j \mathbf{R}_{i,j} \quad (2)$$

$$n_S^i = \arg \max_k \mathbf{R}_{k,n_q^i} \quad (3)$$

$$m^i = \mathbb{1}(i = n_S^i) \quad (4)$$

where $\mathbb{1}$ is the indicator function, when $i = n_S^i$, $\mathbb{1}$ is equal to 1, otherwise it is 0. Using mask m and semantic relation matrix \mathbf{R}_n , we can get sparse attention map a^n and use it to align each support class n to query image q and get task-specific prototype $v_{S_n|q}$, which can be computed as:

$$a_n = m * \mathbf{R}_n \in \mathbb{R}^{K \times MK} \quad (5)$$

$$v_{S_n|q} = a_n \times v_{S_n}^\top \in \mathbb{R}^{K \times C'} \quad (6)$$

A pseudo code of sparse spatial transformers layer in a PyTorch-like style is shown in Algorithm 1.

4.3. Patch Matching Module

Patching matching module is built as a similarity metric, which does not have any parameter to train. Given query value $v_q \in \mathbb{R}^{K \times C'}$ and the aligned prototype of class n $v_{S_n|q} \in \mathbb{R}^{K \times C'}$, we can get their patch-to-patch similarity

Algorithm 1 Pseudo code of sparse spatial transformers layer in a PyTorch-like style

key projection head h_k
query projection head h_q
value projection head h_v

Input: query feature q , support feature S

Output: aligned prototype $v_{S|q}$

support key $\in \mathbb{R}^{N \times C' \times MK}$

$k_S = h_k(S)$

query query $\in \mathbb{R}^{C' \times K}$

$q_q = h_q(q)$

query value $\in \mathbb{R}^{C' \times K}$, support value $\in \mathbb{R}^{N \times C' \times MK}$

$v_q, v_S = h_v(q), h_v(S)$

similarity matrix $\in \mathbb{R}^{N \times K \times MK}$

$\mathbf{R} = q_q.\text{unsqueeze}(0).\text{transpose}(-1, -2) \times k_S$

max index $q_q^{max} \in \mathbb{R}^K, k_S^{max} \in \mathbb{R}^{NMK}$

$q_q^{max} = \mathbf{R}.\text{permute}(1, 0, 2).\text{view}(K, -1).\text{max}(-1)[1]$

$k_S^{max} = \mathbf{R}.\text{permute}(1, 0, 2).\text{view}(K, -1).\text{max}(-2)[1]$

mask $m \in \mathbb{R}^K$

$m = \text{torch.gather}(k_S^{max}, 0, q_q^{max})$

$m = (m_{q|S} == \text{torch.arange}(K))$

attention map $a \in \mathbb{R}^{N \times K \times MK}$

$a = \mathbf{R} * m.\text{unsqueeze}(0).\text{unsqueeze}(-1)$

$a = \text{dropout}(\text{nn.Softmax}(\text{dim}=-1)(a))$

aligned prototype feature $v_{S|q} \in \mathbb{R}^{N \times K \times C'}$

$v_{S|q} = a \times v_S.\text{transpose}(-1, -2)$

return $v_{S|q}$

matrix by:

$$\mathbf{D}^n = \frac{v_q \times v_{S_n|q}}{\|v_q\| \cdot \|v_{S_n|q}\|} \in \mathbb{R}^{K \times K} \quad (7)$$

Then, for each patch in v_q , we select the most similar patch in all patches from prototype $v_{S_n|q}$. Then, we sum K selected patches as the similarity between the query image and support class n :

$$P^n = \sum_{i=1}^K \max_{j \in \{1, \dots, K\}} \mathbf{D}_{i,j}^n \quad (8)$$

Under the N -way M -shot few-shot learning setting, we can get semantic similarity vectors $P \in \mathbb{R}^N$.

Table 1. Average classification accuracy of 5-way 1-shot and 5-way 5-shot tasks with 95% confidence intervals on *miniImageNet* and *tieredImageNet*. † Results re-implemented by [16]. (Red/blue is best/second best performances)

Method	Venue	Backbone	Type	<i>miniImageNet</i>	
				5-way 1-shot	5-way 5-shot
ProtoNet [22]	NeurIPS'17	Conv-64F	Metric	49.42±0.78	68.20±0.66
CovaMNet [14]	AAAI'19	Conv-64F	Metric	51.19±0.76	67.65±0.63
DN4 [13]	CVPR'19	Conv-64F	Metric	51.24±0.74	71.02±0.64
DSN [21]	CVPR'20	Conv-64F	Metric	51.78±0.96	68.99±0.69
DeepEMD† [27]	CVPR'20	Conv-64F	Metric	52.15±0.28	65.52±0.72
SSFormers	Ours	Conv-64F	Metric	55.00±0.22	70.55±0.17
ProtoNet [22]	NeurIPS'17	ResNet12	Metric	62.59±0.85	78.60±0.16
CAN [10]	NeurIPS'19	ResNet12	Metric	63.85±0.48	79.44±0.34
DSN [21]	CVPR'20	ResNet12	Metric	62.64±0.66	78.83±0.45
DeepEMD [27]	CVPR'20	ResNet12	Metric	65.91±0.82	82.41±0.56
FEAT [26]	CVPR'20	ResNet12	Metric	66.78±0.20	82.05±0.14
RENet [11]	ICCV'21	ResNet12	Metric	67.60±0.44	82.58±0.30
PSST [4]	CVPR'21	ResNet12	Optimization	64.05±0.49	80.24±0.45
GLoFA [17]	AAAI'21	ResNet12	Optimization	66.12±0.42	81.37±0.33
SSFormers	Ours	ResNet12	Metric	67.25±0.24	82.75±0.20

Method	Venue	Backbone	Type	<i>tieredImageNet</i>	
				5-way 1-shot	5-way 5-shot
ProtoNet [22]	NeurIPS'17	Conv-64F	Metric	53.31±0.89	72.69±0.74
CovaMNet [14]	AAAI'19	Conv-64F	Metric	54.98±0.90	71.51±0.75
DN4 [13]	CVPR'19	Conv-64F	Metric	53.37±0.86	74.45±0.70
DSN [21]	CVPR'20	Conv-64F	Metric	53.22±0.66	71.06±0.55
DeepEMD† [27]	CVPR'20	Conv-64F	Metric	50.89±0.30	66.12±0.78
SSFormers	Ours	Conv-64F	Metric	55.54±0.19	73.72±0.21
ProtoNet [22]	NeurIPS'17	ResNet12	Metric	68.37±0.23	83.43±0.16
CAN [10]	NeurIPS'19	ResNet12	Metric	69.89±0.51	84.23±0.37
DSN [21]	CVPR'20	ResNet12	Metric	67.39±0.82	82.85±0.56
FEAT [26]	CVPR'20	ResNet12	Metric	70.80±0.23	84.79±0.16
DeepEMD [27]	CVPR'20	ResNet12	Metric	71.16±0.87	83.95±0.58
RENet [11]	ICCV'21	ResNet12	Metric	71.61±0.51	85.28±0.35
GLoFA [17]	AAAI'21	ResNet12	Optimization	69.75±0.33	83.58±0.42
SSFormers	Ours	ResNet12	Metric	72.52±0.25	86.61±0.18

Table 2. Ablation study on our model, we can find that each part of our model has important contribution. The experiments are conducted with *ResNet12* on *miniImageNet*. (SSTL: Sparse Spatial Transformer Layer and PMM: Patch Matching Module)

Dense Local Feature	SSTL	PMM	Cosine Classifier	5-way 1-shot	5-way 5-shot
	✓	✓		63.15±0.20	79.15±0.25
✓	✓	✓		66.84±0.47	79.72±0.50
✓	✓		✓	64.35±0.22	80.17±0.17
✓	✓	✓		67.25±0.24	82.75±0.20

5. Experiments

To evaluate the effectiveness of our method, we conduct extensive experiments on several common-used bench-

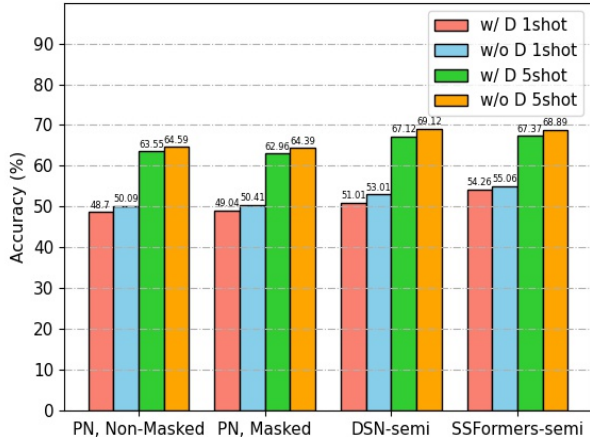


Figure 2. 5-way semi-supervised few-shot learning results on *miniImageNet*. We show the results with (w/ D) and without *distractors*(w/o D). And we compare our methods with PN, Non-Masked [19], PN, Masked [19] and DSN-semi [21].

Table 3. The 5-way, 1-shot and 5-shot classification accuracy (%) with different number of image patches on *miniImageNet*.

Embedding	5-way 1-shot	5-way 5-shot
5×5	65.20 ± 0.24	80.07 ± 0.26
4×4	66.37 ± 0.23	81.06 ± 0.25
3×3	65.17 ± 0.22	81.69 ± 0.20
2×2	65.18 ± 0.22	80.10 ± 0.16
$4 \times 4 + 3 \times 3$	66.08 ± 0.24	81.50 ± 0.26
$4 \times 4 + 2 \times 2$	67.25 ± 0.24	82.75 ± 0.20
$3 \times 3 + 2 \times 2$	67.05 ± 0.22	82.53 ± 0.18

Table 4. The 5-way, 1-shot and 5-shot classification accuracy (%) with different attention methods on *tieredImageNet*.

Method	Self	Cross	1-shot	5-shot
ProtoNet			68.37 ± 0.23	83.43 ± 0.16
CAN		✓	69.89 ± 0.51	84.23 ± 0.37
FEAT		✓	70.80 ± 0.23	84.79 ± 0.16
RENet	✓	✓	71.61 ± 0.51	85.28 ± 0.35
SSFormers		✓	72.52 ± 0.25	86.61 ± 0.18

marks for few-shot image recognition. In this section, we first present details about datasets and experimental settings in our network design. Then, we compare our method with the state-of-the-art methods on various few-shot learning tasks, i.e., standard few-shot learning, cross-domain few-shot learning. Finally, we conduct comprehensive ablation studies to validate each component in our network.

Table 5. Stability evaluation on *miniImageNet*. Comparison with Rethink-Distill [24].

+ GaussianBlur ($\delta \in [0.1, 2]$)	
Rethink-Distill	82.14 \rightarrow 49.30
SSFormers	82.75 \rightarrow 77.17
+ pepperNoise ($r = 0.01$)	
Rethink-Distill	82.14 \rightarrow 63.97
SSFormers	82.75 \rightarrow 66.74
+ ColorJitter ($B = 0.8$)	
Rethink-Distill	82.14 \rightarrow 81.05
SSFormers	82.75 \rightarrow 81.21

5.1. Datasets

We conduct few-shot image recognition problems on two popular benchmarks, i.e., *miniImageNet*, *tieredImageNet*.

***miniImageNet*.** *miniImageNet* is a subset random sampled from ImageNet and is an important benchmark in few-shot learning community. *miniImageNet* consists of 60,000 images in 100 categories. We follow the standard partition settings [22], where there are 64/16/20 categories for training, validation and evaluation.

***tieredImageNet*.** *tieredImageNet* is also a subset random sampled from ImageNet, which consists of 779,165 images in 608 categories. All 608 categories are grouped into 34 broader categories. Following the same partition settings [10], we use 20/6/8 broader categories for training, validation, and evaluation respectively.

5.2. Implementation Details

Backbone networks. For fair comparison, following [21], we employ *Conv-64F* and *ResNet12* as our model backbone. To generate pyramid dense features, we add a global average pooling layer at the end of the backbone, such that the backbone generates a vector for each input image patch. And we slightly expand the area of the local patches in the grid by 2 times to merge the context information, which is helpful to generate the local representations.

Training details. The training process can be divided into two stages: pre-training and meta-training. Following [27], we apply a pre-train strategy. The backbone networks are trained on training categories with a softmax layer. In this stage, we apply data augmentation methods to increase the generalization ability of the model, i.e., color jitter, random crop, and random horizontal flip. The backbone network in our model is initialized with pre-trained weights, which are then fine-tuned along with other components in our model. In the meta-training stage, we conduct N -way M -shot tasks on all benchmarks, i.e., 5-way 1-shot and 5-way 5-shot. *Conv-64F* is optimized by Adam, and

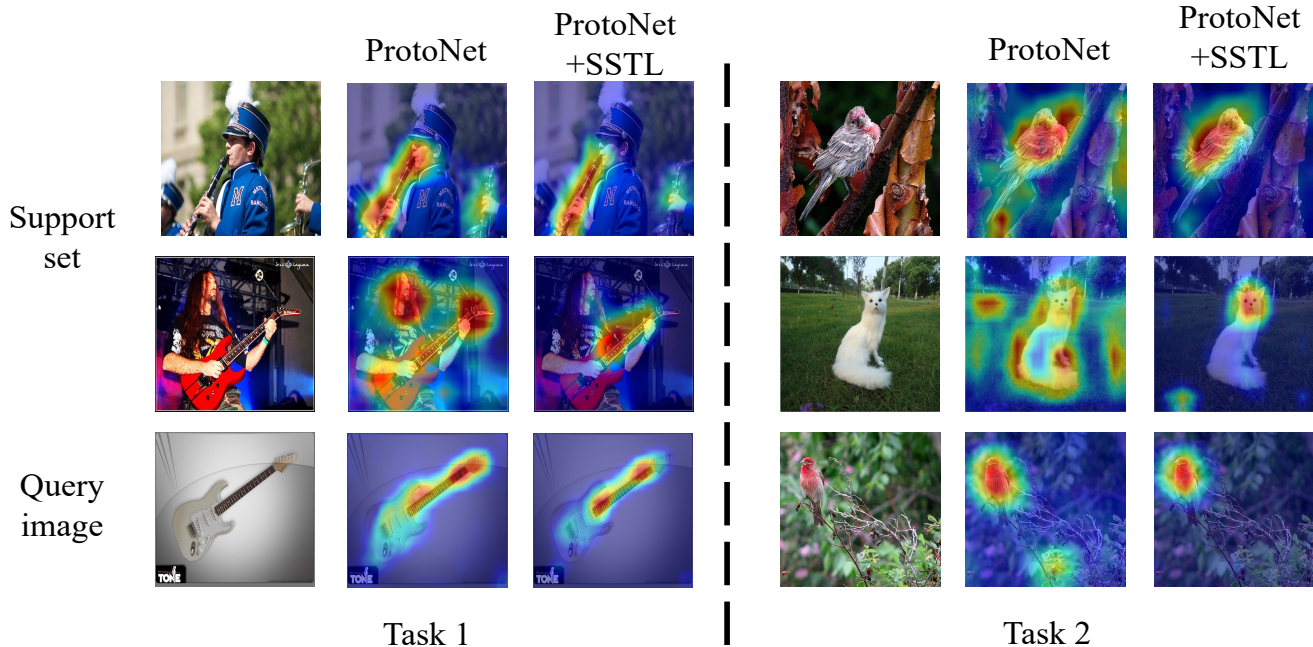


Figure 3. Grad-class activation mapping (Grad-cam) visualization on two 2-way 1-shot tasks. In contrast to ProtoNet, our sparse spatial transformer layer (SSTL) can automatically highlight task-relevant areas.

the initial learning rate is set to 0.1 and decay 0.1 every 10 epochs. And *ResNet12* is optimized by SGD, and the initial learning rate is set to $5e-4$ and decay 0.5 every 10 epochs.

Evaluation. During the test stage, we random sample 10,000 tasks from the meta-testing set, and take averaged top-1 classification accuracy as the performance of methods.

5.3. Standard Few-shot Image Classification

To verify the effectiveness of our proposed SSFormers for few-shot image classification task, we conduct comprehensive experiments and compare our methods with other state-of-the-art methods. The experimental results are shown in Table 1 and Table 2. The results show that our method achieves the best results in almost all settings. For example, compared with the classic attention-based method CAN [10], our model is around 4.4%/4.0% better than CAN on *miniImageNet* with *ResNet12*. And compare with the previous transformers-based method FEAT [26], which uses transformers to find task-specific features in the support set, our method achieves 1.4%/2.0% improvements on *tieredImageNet* with *ResNet12*.

The reason why we can achieve this improvement is that SSFormers can find task-relevant patches in the current task and perform sparse spatial cross attention algorithms based on hierarchical dense representations.

5.4. Semi-supervised Few-Shot Learning

We further verify the effectiveness of our model on more challenging semi-supervised few-shot learning tasks. Under semi-supervised few-shot learning settings, we can select image patches from unlabeled samples that meet the mutual perception function (Eq. (2)-(4)) with the current support set and add them to the support set to provide more support features. Specifically, the workflow of SSFormers-semi is as follows: for the support set n , we first search for all patches that satisfy the mutual perception function in unlabeled sets and put them into the set U_n . Then we use U_n to extend S_n : $S_n = \{S_n^1, \dots, S_n^{MK}\} \cup U_n$. Then, we use the original SSFormers to calculate the similarity.

We use the same experiment setting in [19]. We use *Conv-64F* as our backbone and train SSFormers-semi on 300,000 tasks on *miniImageNet*. The results are shown in Figure 3, where SSFormers-semi shows competitive results with classical baseline methods.

5.5. Ablation Study

Analysis of Our Method. Our model consists of different components: dense local feature extractor, sparse spatial transformer layer, and patch matching module. As shown in Table 2, we studied the effect of each component on the results on the *miniImageNet*. Note that when replacing the patch matching module, we calculate the cosine similarity spatially. The results show that every component in SSFormers has a significant contribution. For example, with-

out our sparse spatial transformer layer, the performance of the model will drop by 3.73% on 5-shot tasks.

Influence of the number of patches. During dividing input images into patches, we have to define the grid for patches. We select various grids and their combinations and conduct analysis experiments on *miniImageNet*. As shown in Table 4, it is better to use a combination of grids of different sizes. A possible explanation is that the size of the main object in different images is different, and the use of a single size may lose context information, and make it difficult to generate high-level semantic representations.

Comparison with other attention methods. As shown in Table 4, our model has achieved state-of-the-art in all attention-based methods. Specifically, compared with ResNet [11], our SSFormers only utilize cross attention, but still leads them in both 1-shot and 5-shot tasks.

Analyze of Stability. A good model should have good robustness and be able to adapt to various environments. For this reason, we tested the stability of our model under three different attacks. As shown in Table 5, the performance of our SSFormers is relatively stable under various attacks.

Qualitative visualizations of the sparse spatial transformer layer. To qualitatively evaluate the proposed sparse spatial transformer layer (SSTL), we provide some visualization cases as shown in Figure 3. We fixed two 2-way 1-shot tasks and used grad-cam [20] to visualize ProtoNet and ProtoNet+SSTL respectively. Specifically, in task 1, ProtoNet highlighted people by mistake, and in task 2, ProtoNet highlighted background information by mistake. On the contrary, ProtoNet+SSTL can correctly highlight the task-relevant areas, which once again verifies the effectiveness of our model.

6. Conclusion

In this work, we proposed a novel sparse spatial transformers (SSFormers) for few-shot learning, which customizes task-specific prototypes via a transformer-based architecture. Specifically, we use image patches to represent images and propose a sparse spatial transformer layer to select task-relevant patches and generate task-specific prototypes. Then we use the patch matching module to calculate similarity scores. Experimental results demonstrate SSFormers can achieve competitive results with other state-of-the-art few-shot learning methods.

References

- [1] Zhe Cao, Gines Hidalgo, Tomas Simon, Shih-En Wei, and Yaser Sheikh. Openpose: Realtime multi-person 2d pose estimation using part affinity fields. *TPAMI*, 43(1):172–186, 2021.
- [2] Haoxing Chen, Huaxiong Li, Yaohui Li, and Chunlin Chen. Multi-scale adaptive task attention network for few-shot learning, 2020.
- [3] Haoxing Chen, Huaxiong Li, Yaohui Li, and Chunlin Chen. Multi-level metric learning for few-shot image recognition, 2021.
- [4] Zhengyu Chen, Jixie Ge, Heshen Zhan, Siteng Huang, and Donglin Wang. Pareto self-supervised training for few-shot learning, 2021.
- [5] Wen-Hsuan Chu, Yu-Jhe Li, Jing-Cheng Chang, and Yu-Chiang Frank Wang. Spot and learn: A maximum-entropy patch sampler for few-shot image classification. In *CVPR*, pages 6251–6260, 2019.
- [6] Carl Doersch, Ankush Gupta, and Andrew Zisserman. Crosstransformers: spatially-aware few-shot transfer. In *NeurIPS*, 2020.
- [7] Chelsea Finn, Pieter Abbeel, and Sergey Levine. Model-agnostic meta-learning for fast adaptation of deep networks. In *ICML*, volume 70, pages 1126–1135, 2017.
- [8] K. Chidananda Gowda and G. Krishna. The condensed nearest neighbor rule using the concept of mutual nearest neighborhood (corresp.). *TIT*, 25(4):488–490, 1979.
- [9] Fusheng Hao, Fengxiang He, Jun Cheng, Lei Wang, Jianzhong Cao, and Dacheng Tao. Collect and select: Semantic alignment metric learning for few-shot learning. In *ICCV*, pages 8459–8468, 2019.
- [10] Ruibing Hou, Hong Chang, Bingpeng Ma, Shiguang Shan, and Xilin Chen. Cross attention network for few-shot classification. In *NeurIPS*, pages 4005–4016, 2019.
- [11] Dahyun Kang, Heeseung Kwon, Juhong Min, and Minsu Cho. Relational embedding for few-shot classification, 2021.
- [12] Aoxue Li, Tiange Luo, Tao Xiang, Weiran Huang, and Liwei Wang. Few-shot learning with global class representations. In *ICCV*, pages 9714–9723, 2019.
- [13] Wenbin Li, Lei Wang, Jinglin Xu, Jing Huo, Yang Gao, and Jiebo Luo. Revisiting local descriptor based image-to-class measure for few-shot learning. In *CVPR*, pages 7260–7268, 2019.
- [14] Wenbin Li, Jinglin Xu, Jing Huo, Lei Wang, Yang Gao, and Jiebo Luo. Distribution consistency based covariance metric networks for few-shot learning. In *AAAI*, pages 8642–8649, 2019.
- [15] Tsung-Yi Lin, Priya Goyal, Ross B. Girshick, Kaiming He, and Piotr Dollár. Focal loss for dense object detection. *IEEE Trans. Pattern Anal. Mach. Intell.*, 42(2):318–327, 2020.
- [16] Yang Liu, Tu Zheng, Jie Song, Deng Cai, and Xiaofei He. DMN4: few-shot learning via discriminative mutual nearest neighbor neural network, 2021.
- [17] Su Lu, Han-Jia Ye, and De-Chuan Zhan. Tailoring embedding function to heterogeneous few-shot tasks by global and local feature adaptors. In *AAAI*, pages 8776–8783, 2021.
- [18] Sachin Ravi and Hugo Larochelle. Optimization as a model for few-shot learning. In *ICLR*, 2017.
- [19] Mengye Ren, Eleni Triantafillou, Sachin Ravi, Jake Snell, Kevin Swersky, Joshua B. Tenenbaum, Hugo Larochelle, and Richard S. Zemel. Meta-learning for semi-supervised few-shot classification. In *ICLR*, 2018.
- [20] Ramprasaath R. Selvaraju, Michael Cogswell, Abhishek Das, Ramakrishna Vedantam, Devi Parikh, and Dhruv Batra. Grad-cam: Visual explanations from deep networks via gradient-based localization. In *ICCV*, pages 618–626, 2017.

- [21] Christian Simon, Piotr Koniusz, Richard Nock, and Mehrtaash Harandi. Adaptive subspaces for few-shot learning. In *CVPR*, pages 4135–4144, 2020.
- [22] Jake Snell, Kevin Swersky, and Richard S. Zemel. Prototypical networks for few-shot learning. In *NeurIPS*, pages 4077–4087, 2017.
- [23] Flood Sung, Yongxin Yang, Li Zhang, Tao Xiang, Philip H. S. Torr, and Timothy M. Hospedales. Learning to compare: Relation network for few-shot learning. In *CVPR*, pages 1199–1208, 2018.
- [24] Yonglong Tian, Yue Wang, Dilip Krishnan, Joshua B. Tenenbaum, and Phillip Isola. Rethinking few-shot image classification: A good embedding is all you need? In *ECCV*, volume 12359, pages 266–282, 2020.
- [25] Oriol Vinyals, Charles Blundell, Tim Lillicrap, Koray Kavukcuoglu, and Daan Wierstra. Matching networks for one shot learning. In *NeurIPS*, pages 3630–3638, 2016.
- [26] Han-Jia Ye, Hexiang Hu, De-Chuan Zhan, and Fei Sha. Few-shot learning via embedding adaptation with set-to-set functions. In *CVPR*, pages 8808–8817, 2020.
- [27] Chi Zhang, Yujun Cai, Guosheng Lin, and Chunhua Shen. Deepemd: Few-shot image classification with differentiable earth mover’s distance and structured classifiers. In *CVPR*, pages 12200–12210, 2020.
- [28] C. Zhang, H. Li, C. Chen, Y. Qian, and X. Zhou. Enhanced group sparse regularized nonconvex regression for face recognition. *TPAMI*, 2020. to be published, doi:10.1109/TPAMI.2020.3033994.